

## Research Article

Esma Nur Gecer\*

# Synthesis and characterization of silver nanoparticles using *Origanum onites* leaves: Cytotoxic, apoptotic, and necrotic effects on Capan-1, L929, and Caco-2 cell lines

<https://doi.org/10.1515/gps-2022-8126>

received October 06, 2022; accepted January 11, 2023

**Abstract:** In this study, *Origanum onites* was used to synthesize the silver nanoparticles (AgNPs@Org). The structure of nanoparticles was identified by spectroscopic techniques. The maximum absorption was determined as 433 nm by UV-Vis spectroscopy. In Fourier-transform infrared spectroscopy spectrum, the characteristic signal was observed at  $3,262\text{ cm}^{-1}$  belonging to the OH group. The crystal structure of nanoparticles was revealed by X-ray diffraction analysis. The diffraction peaks ( $2\theta$ ) can be indexed to 111, 200, 220, 311, and 222 components representing the face-centered cubic unit structure. The spherical particle size was calculated as 18.1 nm by transmission electron microscopy. Cytotoxic effects of extract and AgNPs@Org were executed by MTT assay using Capan-1, L929, and Caco-2 cell lines. AgNPs@Org exhibited the excellent cytotoxic effect on Capan-1 cell lines with the viability of 37.6% ( $0.5\text{ }\mu\text{g}\cdot\text{mL}^{-1}$ ). However, the effect of *O. onites* extract on the viability of Capan-1 cell lines was found to be 24.6% and 55.4% at 1.0 and  $0.5\text{ }\mu\text{g}\cdot\text{mL}^{-1}$ , respectively. AgNPs@Org effect on Caco-2 cell lines was found as 31.7% ( $1.0\text{ }\mu\text{g}\cdot\text{mL}^{-1}$ ). In the L929 cell lines, the noticeable lethal influence was not detected for extract and nanoparticles. In other words, the extract and AgNPs@Org did not act a cytotoxic effect on L929 cell lines.

**Keywords:** silver nanoparticles, spectroscopy, *Origanum onites*, anticancer activity, apoptosis

## 1 Introduction

Nanotechnology is a speedily emerging division of science to produce valuable materials at the nanoscale, which is an effective area of use in science and technology [1]. Nanomaterials have been used effectively in mechanics, optics, pharmaceuticals, chemistry, and medicine in recent years. Natural products have attracted great interest in drugs' development because they do not have significant side effects [2–6].

Natural product-mediated nanoparticle synthesis has made an important contribution to the discovery and development of cancer drugs in recent years. Cancer is a deadly disease, and it is a significant public health problem worldwide [7]. In accordance with the World Health Organization (WHO), cancer is one of the chief reasons of death, reported for 7.6 million deaths (13%) of the world population annually. WHO estimates that the amount of cancer patients will rise to 24 million by 2032. Taking into account the increasing incidence of cancer, it is urgent to control tumor cell growth. Chemotherapy drugs are used effectively in cancer treatment. However, these drugs have high toxicity and side effects [8,9]. Natural products appeared as a robust alternative to synthetic drugs. Moreover, these natural molecules have also been a source of inspiration for the synthesis of many synthetic molecules for cancer treatment [10–12].

Nanoparticles synthesized using natural products will make an important contribution to the development of cancer drugs [13]. The silver nanoparticles synthesized using *Salacia chinensis* displayed significant activity against various cancerous cell lines such as cervical, prostate, lungs, and pancreas [14].

In addition, *Melia dubia* leaf extract was used for silver nanoparticle synthesis, and it showed high cytotoxicity against human breast cancer (KB) cell lines [13]. In addition, Ag–Pt nanoparticles revealed the dose-dependent

\* Corresponding author: Esma Nur Gecer, Department of Chemistry, Faculty of Arts and Sciences, Tokat Gaziosmanpasa University, 60240 Tokat, Turkey, e-mail: esmanurgecer@hotmail.com

anticancer activity against glioblastoma and melanoma cell lines [15]. When AgNPs enter the cancer cell, the redox state is destabilized, and internal homeostasis is lost. Free radicals damage the nuclear membrane and mitochondria. In the DNA replication of the cell cycle, damaged DNA cannot be effectively fixed. Silver ions can block the enzymes to stop the replication [16]. Moreover, silver nanoparticles were reported to reveal considerable antioxidant activity [17–22].

*Origanum* genus, which belongs to the Lamiaceae family, includes aromatic and medicinal plants widely used in the food and pharmaceutical industry [23]. *Origanum* species have been employed commonly in folk medicine to treat various illnesses. Phytochemical studies on *Origanum* species revealed the isolation of bioactive compounds such as terpenoids, flavonoids, and steroids [24–26].

Due to the bioactive compound content of *Origanum onites* [26], it is hypothesized that silver nanoparticles capped and stabilized by related compounds may exhibit biological activities, especially anticancer activity. In this scope, cytotoxic effect of silver nanoparticles was presented using human pancreatic adenocarcinoma cell lines (Capan-1), human colon adenocarcinoma cell line (Caco-2), and mouse normal fibroblast cell lines (L929). This is the first report to present the anticancer activity against corresponding cancerous cell lines of AgNPs@Org synthesized using *O. onites*.

## 2 Materials and methods

### 2.1 Silver nanoparticles synthesis

Silver nanoparticles were synthesized using *O. onites* leaves which was cultivated in Aromatic and Medicinal Plant Field of Tokat Gaziosmanpasa University. The taxonomic identification was executed by Dr. O. Eminagaoglu, Artvin Coruh University, where a voucher specimen was deposited (ARTH 5255). The collection of plant was approved by the Biodiversity Authorization and Information System and the study complies with local and national guidelines [27].

### 2.2 Characterization of silver nanoparticles

The spectroscopic study was employed to identify the silver nanoparticles. The maximum absorption at 433 nm was observed by UV-Vis spectroscopy (UV-2600 Shimadzu spectrophotometer). Fourier-transform infrared (FT/IR-4700

Jasco) spectrometer was utilized to present the functional groups of bioactive compounds responsible for reducing agents. The morphology, size, and shape of the nanostructure were determined by transmission electron microscopy (TEM) analysis (Hitachi HighTech HT7700). X-ray diffraction (XRD) (Empyrean, Malvern Panalytical diffractometer) was used to reveal the crystalline structure.

### 2.3 Cell culture

This research was carried out according to the principles of the Declaration of Helsinki at Hitit University, Scientific Research Center, with the permission of University Council. Human colon adenocarcinoma cell line (Caco-2), human pancreatic adenocarcinoma cell lines (Capan-1), and mouse normal fibroblast cell lines (L929) were supplied from Kirikkale University, Turkiye. Five microliters was taken from the cells in 1.0 mL solution and they were mixed with the trypan blue then and were added to Thoma lam. There were 25 squares in Thoma lam. Five squares were counted randomly. Totally, 25 squares were counted, and then, average values were calculated. Afterward, cell numbers were calculated in 1.0 mL to determine the concentration.

$$\begin{aligned} & \text{Viable cell count} \\ &= \frac{\text{Number live cells counted}}{\text{Number of large corner squares counted}} \quad (1) \\ & \times \text{Dilution factor} \times 10,000 \end{aligned}$$

Anticancer activity of extract and nanoparticles were investigated on these cell lines. The cells were taken from a deep freezer and dissolved (37°C) and moved to tubes (15 mL) in a Laminar cabinet and centrifuged for 5 min. DMEM was added to the cells that were transferred to flasks. The solution was incubated at 37°C for 48 h in a CO<sub>2</sub> atmosphere (5%). Afterward, media was thrown, and cells were treated with trypsin-EDTA and centrifuged at 10,000 rpm for 7 min [28].

### 2.4 MTT assay

The cytotoxic effect of extract and AgNPs@Org were carried out using a 96-well plate. Initially, the cells (100 µL, 10 × 10<sup>3</sup> per well) were located in a media and incubated for 24 h. After removal of the media, AgNPs@Org and extract with several concentrations (1.0–0.125 µg·mL<sup>-1</sup>) were added to the well and then incubated for 24 h. MTT solution (1.0 µg·mL<sup>-1</sup>, 50 µL) was added after the removal of media and the solution was incubated for

3 h at 37°C. Subsequently, MTT solution was changed to the new one. Isopropyl alcohol was used to dissolve the formazan crystals. ELISA was used for the viability of cells at 570 nm. The cell viability of each group was calculated as given in the following equation. The control cell viability was assumed as 100% [29]:

$$\text{Cell viability \%} = [A_x/A_y] \times 100 \quad (2)$$

where  $A_x$  is the sample and  $A_y$  is the control.

## 2.5 Apoptotic and necrotic analysis

Hoechst dye and propidium iodide (PI) were employed for the measurement of apoptotic and necrotic cells. Cells were cultivated in a 48-well plate with penicillin–streptomycin (1%), and fetal bovine serum (10%) for 24 h at 37°C, with 5% CO<sub>2</sub> atmosphere in DMEM. Different concentrations of (1.0–0.125 µg·mL<sup>-1</sup>) extract and nanoparticles were treated with the cells for 24 h, for 20 min at room temperature. Hoechst dye with blue fluorescence was used to stain the normal cell nuclei. Yet, apoptotic cells are stained with stronger fluorescence. Since necrotic cells do not have plasma membrane integrity, PI dye can penetrate their cell membrane. Therefore, the necrotic cell nuclei were stained red by PI. Fluorescence inverted microscopy with DAPI and FITC filters was employed for the assignment of apoptotic and necrotic cells, respectively. One hundred cells are counted from three different area and apoptosis, necrosis, and viable cells are counted and calculated as %. Viable cells are not stained but determine as shade and morphology of viable cells become smooth [30].

## 2.6 Statistical analysis

GraphPad Prism (8.0.1) with one-way analysis of variance was used for statistical analysis. Tukey's multiple comparison test was used to compare each column with the others. The results were stated as mean values ± standard deviations ( $P < 0.05$ ).

# 3 Results and discussion

## 3.1 Synthesis and UV-Vis spectral analysis of silver nanoparticles

Silver nanoparticles were synthesized using *O. onites* leaf extract. Nanoparticle synthesis was proven by the color

change from yellow to dark brown. The absorption in the range of 350–550 nm in UV-Vis spectroscopy is an important indicator of nanoparticle synthesis [31]. So, maximum absorption in UV-Vis spectrum was observed at 433 nm that proved the formation of nanoparticles (Figure 1). After three stages including reduction, clustering, and growth, nanoparticles formed.

## 3.2 Fourier-transform infrared spectroscopy (FTIR)

FTIR spectroscopic study showed the bioactive compounds responsible for the reduction of Ag<sup>1+</sup> ions and stabilization of nanoparticles. The peak at 3,261 cm<sup>-1</sup> belongs to the OH group and 2,931 cm<sup>-1</sup> may be due to the CH stretching. The signal at 1,594 cm<sup>-1</sup> can be designated to the NH bending. The peak at 1,521 cm<sup>-1</sup> can belong to NO stretching. The signal observed at 1,259 cm<sup>-1</sup> can be assigned to CO stretching. The signals at 1,017 and 813 cm<sup>-1</sup> arise from alkene bending and the signal at 521 cm<sup>-1</sup> may be due to the halo compound (Figure 2).

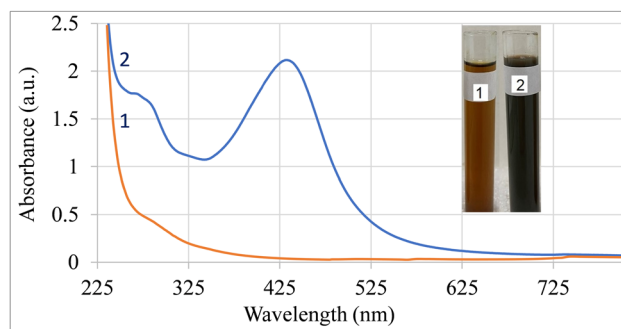


**Figure 1:** UV-Vis spectrum of extract (1) and AgNPs@Org (2). (Inset) The solution of extract (1) and AgNPs (2).

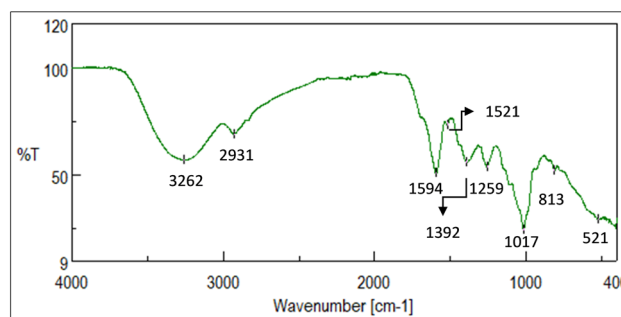


**Figure 2:** FTIR spectrum of extract.

### 3.3 XRD

XRD measurement revealed the crystal structure of green-synthesized nanoparticles (Figure 3). Diffraction peaks at the angle of 38.2, 44.4, 64.7, 77.5, and 81.6° can be indexed to 111, 200, 220, 311, and 222 components representing the face-centered cubic unit structure that agreed with the standard silver card value (JCPDS no. 87-0720) [32].

### 3.4 TEM

The size of nanoparticles is a significant issue since nanoparticles reveal different chemical and physical properties depending on their size and shape. Transmission electron microscopy is one of the best techniques for displaying the size and shape of nanoparticles as well as their distribution. The most TEM studies were executed on green synthesis of silver nanoparticles using plant

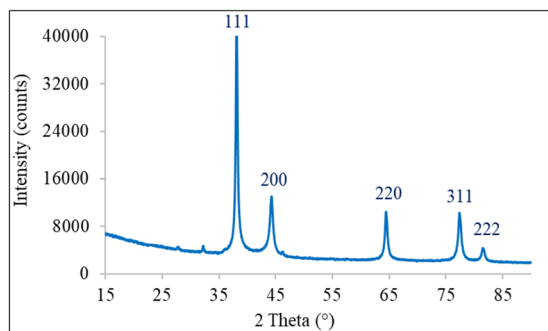


Figure 3: XRD pattern of AgNPs@Org.

extracts [33]. In this study, TEM analysis presented the nanoparticles to be spherical shape. The average particle size of AgNPs@Org was calculated as 18.1 nm (Figure 4).

### 3.5 Cytotoxic activity

Cancer is a deadly disease and extensive scientific studies have been carried out in the discovery and development of anticancer drugs. In this study, the cytotoxic effect of extract and silver nanoparticles were investigated using human pancreatic adenocarcinoma cell lines (Capan-1), mouse normal fibroblast cell lines (L929), and human colon adenocarcinoma cell line (Caco-2) by MTT assay. The first column and second column represent the extract and silver nanoparticles in the figures, respectively. The effect of extract and AgNPs@Org on cell viability in Capan-1 cell lines was determined as 24.6% and 45.4%, respectively ( $1.0 \mu\text{g}\cdot\text{mL}^{-1}$ ) (Figure 5).

This result indicates that the extract is more effective than that of the nanoparticles at a given concentration. However, at  $0.5 \mu\text{g}\cdot\text{mL}^{-1}$ , the effectiveness of nanoparticles is higher than that of the extract. The viability of cells for extract and nanoparticles was detected as 55.4% and 37.6%, respectively, at  $0.5 \mu\text{g}\cdot\text{mL}^{-1}$ . The efficiency of extract and nanoparticles in these cell lines increases due to the increase in concentration. Regarding Caco-2 cell lines (Figure 6), the viability effect of extract and nanoparticles on cell lines was determined as 31.2% and 34.4% at  $0.5 \mu\text{g}\cdot\text{mL}^{-1}$ , respectively. The viability of extract and nanoparticles at  $0.250 \mu\text{g}\cdot\text{mL}^{-1}$  on Caco-2 cells was found as 41.6% and 35.4%, respectively. So, nanoparticles were more effective than that of the extract.

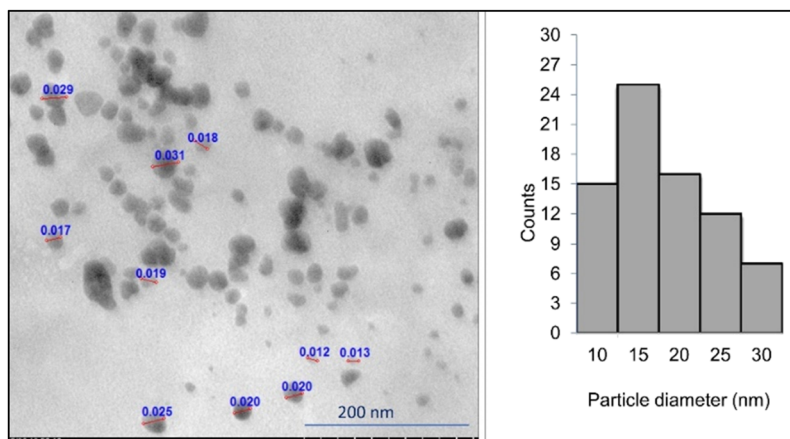
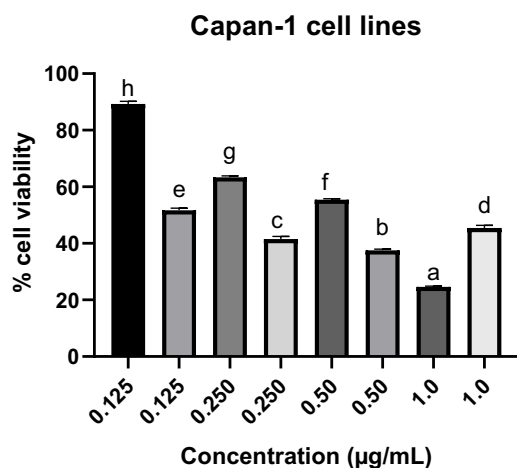
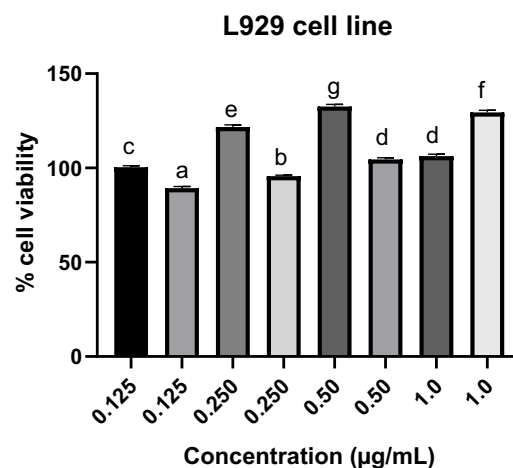


Figure 4: TEM image of AgNPs@Org and particle size distribution.



**Figure 5:** Cytotoxic effect of extract and AgNPs@Org on Capan-1 cell lines. The first and second columns indicate the extract and nanoparticles, respectively. Different letters indicated significantly different ( $p < 0.05$ ) compared in each assay.



**Figure 7:** Cytotoxic effect of extract and AgNPs@Org on L929 cell lines. The first and second columns indicate the extract and nanoparticles, respectively. Different letters indicated significantly different ( $p < 0.05$ ) compared in each assay.

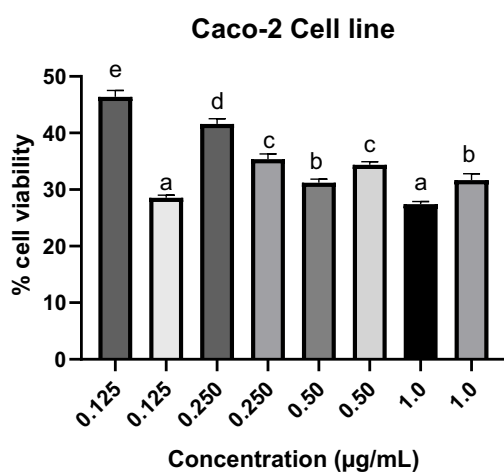


**Figure 6:** Cytotoxic effect of extract and AgNPs@Org on Caco-2 cell lines. The first and second columns indicate the extract and nanoparticles, respectively. Different letters indicated significantly different ( $p < 0.05$ ) compared in each assay.

In L929 cell lines (Figure 7), extract and nanoparticles have no lethal effect on L929 cell lines, which are the mouse normal fibroblast cell lines. That means nanoparticles have no harmful effect on normal cells.

Cell death is required for many biological processes such as development. Furthermore, it contributes to diseases such as cancer. Cell death can be classified into two types: apoptosis and necrosis. Apoptosis is thought to be a physiological form of cell death in which a cell provokes its own death in response to a stimulus. However, necrosis occurs when cells are irreversibly damaged by an external trauma.

The double staining technique was employed to determine the pathway of cell death. Apoptotic index was found higher than that of the necrotic index in Capan-1, Caco-2, and L929 cell lines indicating the cell death in apoptotic pathway (Table 1).

In double staining solution, the Hoechst fluorescent dye bound to DNA and cell nuclei became blue color. Apoptotic cell nuclei were distorted. The necrotic cell nuclei were dyed with PI observed as a red under the fluorescent light. In the control group, any morphological changes were not observed in the cell nuclei (Figure 8). However, apoptotic cells were stained with a strong blue fluorescence. AgNPs had an apoptotic effect in a concentration-dependent manner. This result indicates that the nanoparticles are more effective than the extract at this concentration.

The extract and nanoparticles do not have a considerable cytotoxic effect on mouse fibroblast cell lines (L929), which is desirable. The drugs developed for cancer should be effective against cancer cells and should not harm normal cells. So, nanoparticles synthesized from *O. onites* had a considerable effect against cancer cells and not

**Table 1:** Apoptotic index (A) and necrotic index (N) of AgNPs and extract on cell lines at  $1.0 \mu\text{g}\cdot\text{mL}^{-1}$

Sample	Index	Capan-1	Caco-2	L929
AgNPs	A	$40.5 \pm 2.1$	$25.3 \pm 2.4$	—
	N	$8.9 \pm 1.4$	$7.4 \pm 1.2$	—
Extract	A	$32.4 \pm 1.9$	$28.6 \pm 1.8$	$5.4 \pm 1.2$
	N	$9.1 \pm 2.1$	$12.3 \pm 2.3$	$0.7 \pm 0.1$

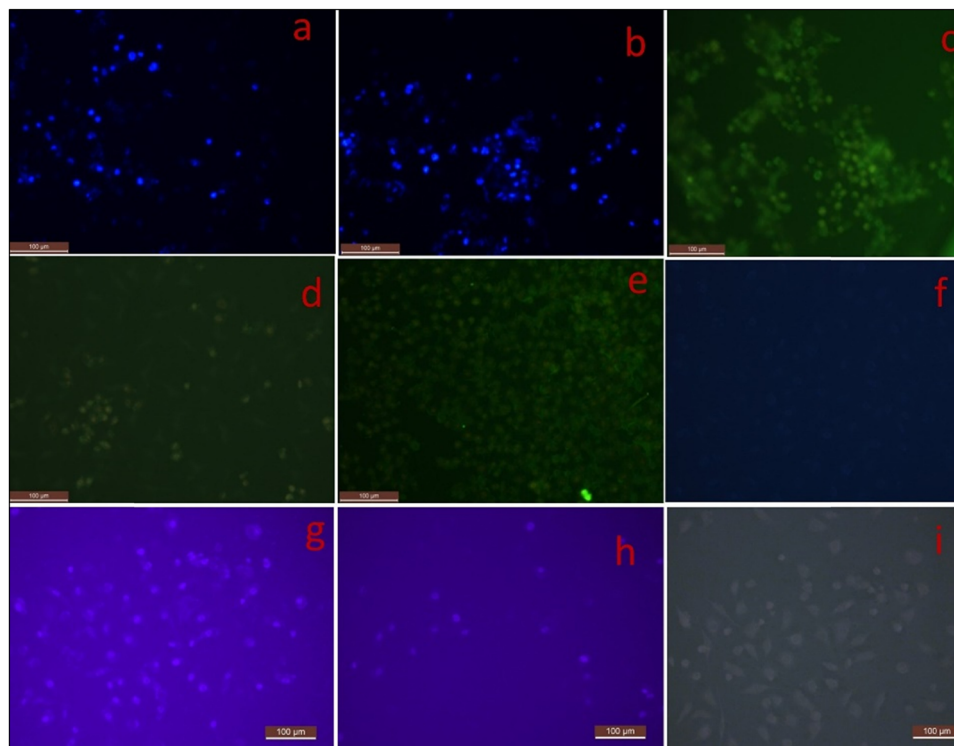


**Figure 8:** Fluorescence inverted microscopy image of Caco-2, extract, and DAPI (a), Caco-2, AgNPs@Org, and DAPI (b), Caco-2 and control (c), L929, extract, and FITC (d), L929, AgNPs@Org, and FITC (e), L929 and control (f), Capan-1, extract, and DAPI (g), Capan-1, AgNPs@Org, and DAPI (h), and Capan-1 and control (i). DAPI images and FITC images showed apoptotic cells and the necrotic cells, respectively.

normal cells. Therefore, AgNPs@Org have the potential to be an anticancer agent. The anticancer activity of nanoparticles was investigated in various studies. Silver nanoparticles were synthesized using *Rheum rhabarbarum* that exhibited anticancer activity against the HeLa cell line [34]. Silver nanoparticles encapsulated by *Taxus baccata* extracts revealed the anticancer effect against human ovarian cancer (Caov-4) and human cervical cancer (HeLa) [35]. Silver and gold nanoparticles were synthesized from *Tussilago farfara* flower and silver nanoparticles revealed the better antibacterial activity than the extract on both Gram-positive and Gram-negative bacteria. Moreover, gold nanoparticles have more cytotoxicity than that of the silver nanoparticles on human pancreas ductal adenocarcinoma cells [36]. The aqueous extract of *S. chinensis* was used to synthesize silver nanoparticles that are non-toxic to normal human fibroblasts and blood erythrocytes, confirming the biocompatibility of green-synthesized silver nanoparticles. Moreover, these nanoparticles demonstrated activity against liver, lungs, pancreas, breast, oral, prostate, and cervical cancer cell lines [14]. In a research, silver nanoparticles were synthesized using aqueous extract of *Origanum vulgare* and these nanoparticles revealed anticancer activity against human lung cancer A549 [37].

## 4 Conclusions

Eco-friendly, low-cost, scalable silver nanoparticles were synthesized using *O. onites*. The characterization of green-synthesized nanoparticles was established extensive spectroscopic study. The spherical shape with the average size of 18.1 nm nanoparticles was obtained. This material revealed the cytotoxic effects against various cancer cell lines. Hence, these nanoparticles could be an effective agent for drug development process. Moreover, nanoparticles could be a promising anticancer agent to overcome insufficient available cancer chemotherapeutics. In this context, the effective and specific activity of the therapeutic agent on cancer cells is very important to reduce the side effects of cancer treatment. The usage of environmentally friendly and natural product methods instead of chemical approaches in the progress of therapeutic agents may also help achievement to this goal. In this study, AgNPs@Org revealed the significant cytotoxic effect on Capan-1 and Caco-2 cell cancerous cell lines, but nanoparticles did not damage to the normal cells and mouse normal fibroblast cell lines, L929. Further *in vivo* study should be carried out to present the potent for anticancer agents.

**Funding information:** Authors state no funding involved.

**Author contributions:** Esmâ Nur Gecer: solely responsible for the entire work.

**Conflict of interest:** The author declares no conflict of interest.

**Data availability statement:** All data generated during this study are included in the manuscript.

## References

- [1] Geetha K, Umadevi M, Sathe GV, Erenler R. Spectroscopic investigations on the orientation of 1,4-dibromonaphthalene on silver nanoparticles. *Spectrochim Acta A Mol Biomol Spectrosc.* 2013;116:236–41. doi: 10.1016/j.saa.2013.07.039.
- [2] Topçu G, Erenler R, Çakmak O, Johansson CB, Çelik C, Chai H-B, et al. Diterpenes from the berries of *Juniperus excelsa*. *Phytochemistry.* 1999;50:1195–9. doi: 10.1016/S0031-9422(98)00675-X.
- [3] Elmastas M, Ozturk L, Gokce I, Erenler R, Aboul-Enein HY. Determination of antioxidant activity of marshmallow flower (*Althaea officinalis* L.). *Anal Lett.* 2004;37:1859–69. doi: 10.1081/AL-120039431.
- [4] Elmastaş M, Telci İ, Akşit H, Erenler R. Comparison of total phenolic contents and antioxidant capacities in mint genotypes used as spices/Baharat olarak kullanılan nane genotiplerinin toplam fenolik içerikleri ve antioksidan kapasitelerinin karşılaştırılması. *Turk J Biochem.* 2015;40:456–62. doi: 10.1515/tjb-2015-0034.
- [5] Erenler R, Sen O, Yaglioglu AS, Demirtas I. Bioactivity-guided isolation of antiproliferative sesquiterpene lactones from *Centaurea solstitialis* l. ssp. *solstitialis*. *Comb Chem High T Scr.* 2016;19:66–72. doi: 10.2174/1386207319666151203002117.
- [6] Guzel A, Aksit H, Elmastas M, Erenler R. Bioassay-guided isolation and identification of antioxidant flavonoids from *Cyclotrichium origanifolium* (Labill.) Manden. and Scheng. *Pharmacogn Mag.* 2017;13:316. doi: 10.4103/0973-1296.204556.
- [7] Ökten S, Çakmak O, Erenler R, Yüce Ö, Tekin S. Simple and convenient preparation of novel 6,8-disubstituted quinoline derivatives and their promising anticancer activities. *Turk J Chem.* 2013;37:896–908. doi: 10.3906/kim-1301-30.
- [8] Demain AL, Vaishnav P. Natural products for cancer chemotherapy. *Microb Biotechnol.* 2011;4:687–99. doi: 10.1111/j.1751-7915.2010.00221.x.
- [9] Reddy L, Odhav B, Bhoola K. Natural products for cancer prevention: a global perspective. *Pharmacol Ther.* 2003;99:1–13. doi: 10.1016/S0163-7258(03)00042-1.
- [10] Sahin Yaglioglu A, Akdulum B, Erenler R, Demirtas I, Telci I, Tekin S. Antiproliferative activity of pentadeca-(8E, 13Z) dien-11-yn-2-one and (E)-1,8-pentadecadiene from *Echinacea pallida* (Nutt.) Nutt. roots. *Med Chem Res.* 2013;22:2946–53. doi: 10.1007/s00044-012-0297-2.
- [11] Erenler R, Pabuccu K, Yaglioglu AS, Demirtas I, Gul F. Chemical constituents and antiproliferative effects of cultured *Mougeotia nummuloïdes* and *Spirulina major* against cancerous cell lines. *Z Naturforsch C.* 2016;71:87–92. doi: 10.1515/znc-2016-0010.
- [12] Erenler R, Sen O, Aksit H, Demirtas I, Yaglioglu AS, Elmastas M, et al. Isolation and identification of chemical constituents from *Origanum majorana* and investigation of antiproliferative and antioxidant activities. *J Sci Food Agr.* 2016;96:822–36. doi: 10.1002/jsfa.7155.
- [13] Kathiravan V, Ravi S, Ashokkumar S. Synthesis of silver nanoparticles from *Melia dubia* leaf extract and their in vitro anticancer activity. *Spectrochim Acta A Mol Biomol Spectrosc.* 2014;130:116–21. doi: 10.1016/j.saa.2014.03.107.
- [14] Jadhav K, Deore S, Dhamecha D, Rajeshwari HR, Jagwani S, Jalalpure S, et al. Phytosynthesis of silver nanoparticles: Characterization, biocompatibility studies, and anticancer activity. *ACS Biomater Sci Eng.* 2018;4:892–9. doi: 10.1021/acsbmaterials.7b00707.
- [15] Ruiz AL, Garcia CB, Gallon SN, Webster TJ. Novel silver-platinum nanoparticles for anticancer and antimicrobial applications. *Int J Nanomed.* 2020;15:169–79. doi: 10.2147/ijn.S176737.
- [16] Sabharwal SS, Schumacker PT. Mitochondrial ROS in cancer: initiators, amplifiers or an Achilles' heel? *Nat Rev Cancer.* 2014;14:709–21. doi: 10.1038/nrc3803.
- [17] Gecer EN. Green synthesis of silver nanoparticles from *Salvia aethiopsis* L. and their antioxidant activity. *J Inorg Organomet Polym Mater.* 2021;31:4402–9. doi: 10.1007/s10904-021-02057-3.
- [18] Gecer EN, Erenler R, Temiz C, Genc N, Yildiz I. Green synthesis of silver nanoparticles from *Echinacea purpurea* (L.) Moench with antioxidant profile. *Part Sci Technol.* 2021;40:50–7. doi: 10.1080/02726351.2021.1904309.
- [19] Genc N, Yildiz I, Chaoui R, Erenler R, Temiz C, Elmastas M. Biosynthesis, characterization and antioxidant activity of oleuropein-mediated silver nanoparticles. *Inorg Nano-Met Chem.* 2021;51:411–9. doi: 10.1080/24701556.2020.1792495.
- [20] Erenler R, Dag B. Biosynthesis of silver nanoparticles using *Origanum majorana* L. and evaluation of their antioxidant activity. *Inorg Nano-Met Chem.* 2022;52:485–92. doi: 10.1080/24701556.2021.1952263.
- [21] Erenler R, Geçer EN. Green synthesis of silver nanoparticles from *Astragalus logopodioides* L. leaves. *Turk J Agricul Food Sci Tech.* 2022;10:1112–5. doi: 10.24925/turjaf.v10i6.1112-1115.5190.
- [22] Geçer EN, Erenler R. Biosynthesis of silver nanoparticles using *Dittrichia graveolens* (Asteraceae) leaves extract: characterisation and assessment of their antioxidant activity. *Turk J Biodiv.* 2022;5:50–6. doi: 10.38059/biodiversity.1090549.
- [23] Erenler R, Adak T, Karan T, Elmastas M, Yildiz I, Aksit H, et al. Chemical Constituents isolated from *Origanum solymicum* with Antioxidant activities. *Eurasia Proceed Sci Tech Eng Math.* 2017;1:139–45.
- [24] Erenler R, Meral B, Sen O, Elmastas M, Aydin A, Eminagaoglu O, et al. Bioassay-guided isolation, identification of compounds from *Origanum rotundifolium* and investigation of their antiproliferative and antioxidant activities. *Pharm Biol.* 2017;55:1646–53. doi: 10.1080/13880209.2017.1310906.

- [25] Elmastas M, Celik SM, Genc N, Aksit H, Erenler R, Gulcin İ. Antioxidant activity of an anatolian herbal tea—*Origanum minutiflorum*: isolation and characterization of its secondary metabolites. *Int J Food Prop*. 2018;21:374–84. doi: 10.1080/10942912.2017.1416399.
- [26] Erenler R, Demirtas I, Karan T, Gul F, Kayir O, Karakoc OC. Chemical constituents, quantitative analysis and insecticidal activities of plant extract and essential oil from *Origanum onites* L. *Trends Phytochem Res*. 2018;2:91–6.
- [27] Sahin Yaglioglu A, Erenler R, Gecer EN, Genc N. Biosynthesis of silver nanoparticles using *Astragalus flavescens* leaf: Identification, antioxidant activity, and catalytic degradation of methylene blue. *J Inorg Organomet Polym Mater*. 2022;32:3700–7. doi: 10.1007/s10904-022-02362-5.
- [28] Karan T, Erenler R. Fatty acid constituents and anticancer activity of *Cladophora fracta* (OF Müller ex Vahl) Kützing. *Trop J Pharm Res*. 2018;17:1977–82. doi: 10.4314/tjpr.v17i10.12.
- [29] Yildiz I, Sen O, Erenler R, Demirtas I, Behcet L. Bioactivity-guided isolation of flavonoids from *Cynanchum acutum* L. subsp. *sibiricum* (willd.) Rech. f. and investigation of their antiproliferative activity. *Nat Prod Res*. 2017;31:2629–33. doi: 10.1080/14786419.2017.1289201.
- [30] Karan T, Erenler R, Bozer BM. Synthesis and characterization of silver nanoparticles using curcumin: cytotoxic, apoptotic, and necrotic effects on various cell lines. *Z Naturforsch C*. 2022;77:343–50. doi: 10.1515/znc-2021-0298.
- [31] Zuas O, Hamim N, Sampora Y. Bio-synthesis of silver nanoparticles using water extract of *Myrmecodia pendan* (Sarang Semut plant). *Mater Lett*. 2014;123:156–9. doi: 10.1016/j.matlet.2014.03.026.
- [32] Beyene HD, Werkneh AA, Bezabh HK, Ambaye TG. Synthesis paradigm and applications of silver nanoparticles (AgNPs), a review. *Sust Mat Technol*. 2017;13:18–23. doi: 10.1016/j.susmat.2017.08.001.
- [33] Rauwel P, Küünal S, Ferdov S, Rauwel E. A review on the green synthesis of silver nanoparticles and their morphologies studied via TEM. *Adv Mater Sci Eng*. 2015;2015:682749. doi: 10.1155/2015/682749.
- [34] Palem RR, Ganesh SD, Kronekova Z, Slavikova M, Saha N, Saha P. Green synthesis of silver nanoparticles and biopolymer nanocomposites: a comparative study on physico-chemical, antimicrobial and anticancer activity. *Bull Mater Sci*. 2018;41:55. doi: 10.1007/s12034-018-1567-5.
- [35] Kajani AA, Zarkesh-Esfahani SH, Bordbar A-K, Khosropour AR, Razmjou A, Kardi M. Anticancer effects of silver nanoparticles encapsulated by *Taxus baccata* extracts. *J Mol Liq*. 2016;223:549–56. doi: 10.1016/j.molliq.2016.08.064.
- [36] Lee YJ, Song K, Cha SH, Cho S, Kim YS, Park Y. Sesquiterpenoids from *Tussilago farfara* flower bud extract for the eco-friendly synthesis of silver and gold nanoparticles possessing antibacterial and anticancer activities. *Nanomaterials*. 2019;9:819. doi: 10.3390/nano9060819.
- [37] Sankar R, Karthik A, Prabu A, Karthik S, Shivashangari KS, Ravikumar V. *Origanum vulgare* mediated biosynthesis of silver nanoparticles for its antibacterial and anticancer activity. *Colloids Surf B Biointerfaces*. 2013;108:80–4. doi: 10.1016/j.colsurfb.2013.02.033.